Inorg. Chem. **2005**, *44*, 7943–7950

Eilatin Complexes of Ruthenium and Osmium. Synthesis, Electrochemical Behavior, and Near-IR Luminescence

Sheba D. Bergman,[†] Dalia Gut,[†] Moshe Kol,*[,†] Cristiana Sabatini,[‡] Andrea Barbieri,[‡] and Francesco Barigelletti*[,‡]

The School of Chemistry, Raymond and Beverly Sackler Faculty of Exact Sciences, Tel Aviv University, Tel Aviv 69978, Israel, and Istituto per la Sintesi Organica e Fotoreattività (ISOF), Consiglio Nazionale delle Ricerche (CNR), Via P. Gobetti 101, 40129 Bologna, Italy

Received June 22, 2005

The synthesis and characterization of new Ru(II) and Os(II) complexes of the ligand eilatin (**1**) are described. The new complexes $[Ru(bpy)(eil)_2]^{2+}$ (**2**), $[Ru(eil)_3]^{2+}$ (**3**), and $[Os(eil)_3]^{2+}$ (**4**) (bpy = 2,2′-bipyridine; eil = eilatin) were synthesized and characterized by NMR, fast atom bombardment mass spectrometry, and elemental analysis. In the series of complexes $[Ru(bpy)_x(eil)_y]^{2+}$ ($x + y = 3$), the effect of sequential substitution of eil for bpy on the electrochemical and photophysical properties was examined. The absorption spectra of the complexes exhibit several bpy- and eil-associated $\pi-\pi^*$ and metal-to-ligand charge-transfer (MLCT) transitions in the visible region (400–600 nm), whose energy and relative intensity depend on the number of ligands bound to the metal center (x and y). On going from $[Ru(bpy)_2(eil)]^{2+}$ (**5**) to **2** to **3**, the $d_\pi(Ru) \rightarrow \pi^*(eil)$ MLCT transition undergoes a red shift from 583 to 591 to 599 nm, respectively. Electrochemical measurements performed in dimethyl sulfoxide reveal several ligand-based reduction processes, where each eil ligand can accept up to two electrons at potentials that are significantly anodically shifted (by ca. 1 V) with respect to the bpy ligands. The complexes exhibit near-IR emission (900–1100 nm) of typical ^{3}MLCT character, both at room temperature and at 77 K. Along the series **5**, **2**, and **3**, upon substitution of eil for bpy, the emission maxima undergo a blue shift and the quantum yields and lifetimes increase. The radiative and nonradiative processes that contribute to deactivation of the excited level are discussed in detail.

Introduction

Octahedral polypyridyl complexes of Ru(II) and Os(II) have attracted substantial scientific interest because of their useful absorption and emission characteristics, their chemical stabilities, and their low barriers to electron and energy transfer.[1−8] The photophysics, photochemistry, and redox behavior of these complexes are ligand-dependent and therefore can be tuned by judicious choice of the ligands bound to the metal center.[9−17] Accordingly, much effort has been focused on structural variations of common ligands such as 2,2′-bipyridine (bpy) and 1,10-phenanthroline (phen), where changing the electronic and steric properties of the

* To whom correspondence should be addressed. E-mail: moshekol@post.tau.ac.il (M.K.), franz@isof.cnr.it (F.B.).
[†] Tel Aviv University.
[‡] Consiglio Nazionale delle Ricerche.

(1) Juris, A.; Balzani, V.; Barigelletti, F.; Campagna, S.; Belser, P.; von Zelewsky, A. *Coord. Chem. Rev.* **1988**, *84*, 85.
(2) Balzani, V.; Juris, A.; Venturi, M.; Campagna, S.; Serroni, S. *Chem. Rev.* **1996**, *96*, 759.
(3) Balzani, V.; Scandola, F. *Supramolecular Photochemistry*; Ellis Horwood: New York, 1991.
(4) Kalyanasundaram, K.; Graetzel, M. *Coord. Chem. Rev.* **1998**, *177*, 347.
(5) Balzani, V.; Juris, A. *Coord. Chem. Rev.* **2001**, *211*, 97.
(6) Ortmans, I.; Moucheron, C.; Kirsch-De Mesmaeker, A. *Coord. Chem. Rev.* **1998**, *168*, 233.
(7) Endicott, J. F.; Schlegel, H. B.; Uddin, M. J.; Seniveratne, D. S. *Coord. Chem. Rev.* **2002**, *229*, 95.
(8) McCusker, J. K. *Acc. Chem. Res.* **2003**, *36*, 876.
(9) Gorelsky, S. I.; Dodsworth, E. S.; Lever, A. B. P.; Vlcek, A. A. *Coord. Chem. Rev.* **1998**, *174*, 469.
(10) Ernst, S. D.; Kaim, W. *Inorg. Chem.* **1989**, *28*, 1520.
(11) Albano, G.; Belser, P.; Daul, C. *Inorg. Chem.* **2001**, *40*, 1408.
(12) Anderson, P. A.; Keene, F. R.; Meyer, T. J.; Moss, J. A.; Strouse, G. F.; Treadway, J. A. *J. Chem. Soc., Dalton Trans.* **2002**, 3820.
(13) Brandt, P.; Norrby, T.; Akermark, E.; Norrby, P. O. *Inorg. Chem.* **1998**, *37*, 4120.
(14) Barigelletti, F.; Juris, A.; Balzani, V.; Belser, P.; von Zelewsky, A. *Inorg. Chem.* **1987**, *26*, 4115.
(15) Treadway, J. A.; Loeb, B.; Lopez, R.; Anderson, P. A.; Keene, F. R.; Meyer, T. J. *Inorg. Chem.* **1996**, *35*, 2242.
(16) Lever, A. B. P. *Inorg. Chem.* **1990**, *29*, 1271.
(17) Vlcek, A. A.; Dodsworth, E. S.; Pietro, W. J.; Lever, A. B. P. *Inorg. Chem.* **1995**, *34*, 1906.

10.1021/ic051022v CCC: $30.25
Published on Web 09/17/2005

ligands ultimately leads to modification of the properties of the resultant complexes.[10,18] Good π-acceptor ligands bearing a low-lying π^* orbital can lead to red-shifting of the metal-to-ligand charge-transfer (MLCT) absorption bands. However, the decreased energy gap between the ground state and the excited state can concomitantly lead to reduction of the excited-state lifetime. This effect is described quantitatively by the energy-gap law, which predicts that, in the absence of competing events, the nonradiative decay rate constant should vary exponentially with the energy gap for a common acceptor ligand.[19−26]

Recently, we have described the employment of eilatin-type ligands in octahedral Ru(II) and Os(II) complexes.[27−34] Eilatin (**1**) combines several unique features: (a) a large, planar fused-aromatic surface of C_{2v} symmetry; (b) two distinct binding sites, a bpy-type "head" and a biq-type "tail" (biq = 2,2′-biquinoline); and (c) a low-lying π^* orbital, which renders it an exceptionally good π-acceptor ligand.[27] We have demonstrated that, in the preparation of complexes of the general formula $[M(N-N)_2(eil)]^{2+}$ (M = Ru, Os; N−N = bpy, phen, biq; eil = eilatin), the eil ligand selectively binds to the metal center via its less sterically hindered bpy-type "head" in the sterically demanding environment provided by the peripheral N−N ligands.[27,28] Moreover, these complexes exhibit a unique low-energy absorption (ca. 600 nm) attributed to a $d_\pi(M) \rightarrow \pi^*$(eil) MLCT transition, as well as anodically shifted reduction potentials of the eil ligand.[29] In addition, these complexes form discrete dimers in solution and in the solid state via intermolecular $\pi-\pi$ interactions between the eil moieties, the extent of which depends on the steric bulk provided by the peripheral N−N ligands bound to the metal center.[28] Because all of these properties arise from the presence of a single eil ligand, we wanted to investigate the effect of sequential replacement of bpy ligands by eil ligands on the properties of such complexes. We report herein the synthesis, NMR characterization, electrochemical behavior, and photophysical properties (from electronic absorption and emission spectroscopy) of the new bis(eilatin) complex $[Ru(bpy)(eil)_2][PF_6]_2$ (**2**) and of the new tris(eilatin) complexes $[Ru(eil)_3][PF_6]_2$ (**3**) and $[Os(eil)_3][PF_6]_2$ (**4**). The emission of these complexes falls in the near-IR region, an occurrence still uncommon for ruthenium(II) polypyridine complexes.[35,36] A detailed discussion concerning radiative and nonradiative processes that contribute to deactivation of the excited level is provided.

Experimental Section

Materials. Eilatin (eil, **1**),[37] $[Ru(bpy)Cl_3]_n$,[38] *trans*-$[RuCl_2(py)_4]$ (py = pyridine),[39] *trans*-$[RuCl_2(DMSO)_4]$ (DMSO = dimethyl sulfoxide),[40] *trans*-$[OsCl_2(py)_4]$,[41] and *trans*-$[OsCl_2(DMSO)_4]$[42] were synthesized according to literature procedures. Ruthenium(III) chloride hydrate (Strem Chemicals), potassium hexachloroosmate(IV) (Pressure Chemical Co.), tetra-*n*-butylammonium hexafluorophosphate (TBAH; 98%, Aldrich), and silver nitrate (99.995%, Aldrich) were used without further purification. Acetonitrile for photophysical experiments was of spectroscopic grade. All other chemicals and solvents were of reagent grade and used without further purification, except for DMSO for electrochemical measurements, which was vacuum distilled over CaH_2. All of the reactions and electrochemical measurements were performed under an argon atmosphere.

Instrumentation. ^1H and ^{13}C NMR spectra, COSY, NOESY, and HMQC experiments were performed on a Bruker Avance 400 spectrometer and on a Bruker ARX-500 spectrometer using the residual protons of the solvent (CD_3CN or DMSO-d_6) as an internal standard at δ = 1.93 and 2.5 ppm, respectively. Fast atom bombardment mass spectrometry (FABMS) spectra were obtained on a VG-AutoSpec M250 mass spectrometer, in a *m*-nitrobenzyl alcohol matrix. Elemental analyses were performed in the microanalytical laboratory in the Hebrew University of Jerusalem. UV/vis absorption spectra in acetonitrile were obtained on a Kontron UVIKRON 931 UV/vis spectrometer.

Cyclic and square-wave voltammograms were carried out on a μ-autolab type II potentiostat (Eco Chemie), using a platinum working electrode, a platinum auxiliary electrode, and a $Ag/AgNO_3$ reference electrode (Bioanalytical Systems). The measurements were carried out on the complexes dissolved in argon-purged DMSO

(18) For example, see: (a) Mabrouk, P. A.; Wrighton, M. S. *Inorg. Chem.* **1986**, *25*, 526. (b) Anderson, P. A.; Deacon, G. B.; Haarmann, K. H.; Keene, F. R.; Meyer, T. J.; Reitsma, D. A.; Skelton, B. W.; Strouse, G. F.; Thomas, N. C.; Treadway, J. A.; White, A. H. *Inorg. Chem.* **1995**, *34*, 6145. (c) Belser, P.; von Zelewsky, A. *Helv. Chim. Acta* **1980**, *63*, 1675. (d) Ernst, S. D.; Kaim, W. *Inorg. Chem.* **1982**, *28*, 1520. (e) Rillema, D. P.; Blanton, C. B.; Shaver, R. J.; Jackman, D. C.; Boldaji, M.; Bundy, S.; Worl, L. A.; Meyer, T. J. *Inorg. Chem.* **1992**, *31*, 1600. (f) Carlson, B.; Phelan, G. D.; Kaminsky, W.; Dalton, L.; Jiang, X.; Liu, S.; Jen, A. K.-Y. *J. Am. Chem. Soc.* **2002**, *124*, 14162. (g) Islam, A.; Ikeda, N.; Yoshimura, A.; Ohno, T. *Inorg. Chem.* **1998**, *37*, 3093.
(19) Englman, R.; Jortner, J. *Mol. Phys.* **1970**, *18*, 145.
(20) Caspar, J. V.; Kober, E. M.; Sullivan, B. P.; Meyer, T. J. *J. Am. Chem. Soc.* **1982**, *104*, 630.
(21) Caspar, J. V.; Meyer, T. J. *Inorg. Chem.* **1983**, *22*, 2444.
(22) Caspar, J. V.; Meyer, T. J. *J. Phys. Chem.* **1983**, *87*, 952.
(23) Kober, E. M.; Caspar, J. V.; Lumpkin, R. S.; Meyer, T. J. *J. Phys. Chem.* **1986**, *90*, 3722.
(24) Chen, P. Y.; Duesing, R.; Tapolsky, G.; Meyer, T. J. *J. Am. Chem. Soc.* **1989**, *111*, 8305.
(25) Chen, P. Y.; Duesing, R.; Graff, D. K.; Meyer, T. J. *J. Phys. Chem.* **1991**, *95*, 5850.
(26) Chen, P. Y.; Mecklenburg, S. L.; Duesing, R.; Meyer, T. J. *J. Phys. Chem.* **1993**, *97*, 6811.
(27) Rudi, A.; Kashman, Y.; Gut, D.; Lellouche, F.; Kol, M. *Chem. Commun.* **1997**, 17.
(28) Gut, D.; Rudi, A.; Kopilov, J.; Goldberg, I.; Kol, M. *J. Am. Chem. Soc.* **2002**, *124*, 5449.
(29) Gut, D.; Goldberg, I.; Kol, M. *Inorg. Chem.* **2003**, *42*, 3483.
(30) Bergman, S. D.; Reshef, D.; Groysman, S.; Goldberg, I.; Kol, M. *Chem. Commun.* **2002**, 2374.
(31) Bergman, S. D.; Reshef, D.; Frish, L.; Cohen, Y.; Goldberg, I.; Kol, M. *Inorg. Chem.* **2004**, *43*, 3792.
(32) Bergman, S. D.; Goldberg, I.; Barbieri, A.; Barigelletti, F.; Kol, M. *Inorg. Chem.* **2004**, *43*, 2355.
(33) D'Alessandro, D. M.; Keene, F. R.; Bergman, S. D.; Kol, M. *Dalton Trans.* **2005**, 332.
(34) Bergman, S. D.; Kol, M. *Inorg. Chem.* **2005**, *44*, 1647.
(35) Treadway, J. A.; Strouse, G. F.; Ruminski, R. R.; Meyer, T. J. *Inorg. Chem.* **2001**, *40*, 4508.
(36) Draper, S. M.; Gregg, D. J.; Schofield, E. R.; Browne, W. R.; Duati, M.; Vos, J. G.; Passaniti, P. *J. Am. Chem. Soc.* **2004**, *126*, 8694.
(37) Gellerman, G.; Rudi, A.; Kashman, Y. *Tetrahedron* **1994**, *50*, 12959.
(38) Krause, R. A. *Inorg. Chim. Acta* **1977**, *22*, 209.
(39) Nagao, H.; Nishimura, H.; Kitanaka, Y.; Howell, F. S.; Mukaida, M.; Kakihana, H. *Inorg. Chem.* **1990**, *29*, 1693.
(40) Evans, I. P.; Spencer, A.; Wilkinson, G. *J. Chem. Soc., Dalton Trans.* **1973**, 204.
(41) Champness, N. R.; Levason, W.; Mould, R. A. S.; Pletcher, D.; Webster, M. *J. Chem. Soc., Dalton Trans.* **1991**, 2777.
(42) da Silva, M.; Pombeiro, A. J. L.; Geremia, S.; Zangrando, E.; Calligaris, M.; Zinchenko, A. V.; Kukushkin, V. Y. *J. Chem. Soc., Dalton Trans.* **2000**, *8*, 1363.

containing 0.1 M TBAH as the supporting electrolyte. The typical concentration of the complexes was ca. 1.5 mM. The criteria for reversibility were the separation between the cathodic and anodic peaks (not exceeding 90 mV), the close-to-unity ratio of the intensities of the cathodic and anodic peak currents, and the constancy of the peak potential on changing scan rate. A 5 mM solution of ferrocene in DMSO containing 0.1 M TBAH was measured after the measurement of each complex, typically yielding a value of $E_{1/2} = 0.039$ V for Fc/Fc^+ vs $Ag/AgNO_3$. Values are reported vs the Fc/Fc^+ couple.

The luminescence spectra for ca. 2×10^{-5} M degassed and air-equilibrated acetonitrile solutions (in this concentration, no dimers due to $\pi-\pi$ stacking of eilatin were observed, in contrast to what was observed for the 1 mM solution of the NMR measurements) at room temperature and 77 K were measured using an Edinburgh FLS920 spectrometer equipped with a Hamamatsu R5509-72 supercooled photomultiplier tube (193 K), a TM300 emission monochromator with near-IR grating blazed at 1000 nm, and an Edinburgh Xe900 450-W xenon arc lamp as the light source. The excitation wavelength was 460 nm, which leads to final population of the lowest-lying emitting levels of Ru- or Os-based MLCT nature (see the Results and Discussion section).[43] Corrected luminescence spectra in the range 700−1800 nm were obtained by using a correction curve for the phototube response provided by the manufacturer. Luminescence quantum yields (Φ) were evaluated by comparing wavelength-integrated intensities (I) with reference to $[Ru(bpy)_3]Cl_2$ ($\Phi_r = 0.028$ in air-equilibrated water)[44] or $[Os(bpy)_3](PF_6)_2$ ($\Phi_r = 0.005$ in degassed acetonitrile)[23] as standards (r = reference) and by using the following equation:[23,45]

$$\Phi = \frac{A_r n^2 I}{n_r^2 I_r A}\Phi_r \qquad (1)$$

where A and n are absorbance values (<0.15) at the employed excitation wavelength and the refractive index of the solvent, respectively. Band maxima and relative luminescence intensities were obtained with uncertainties of 2 nm and 20%, respectively. The luminescence lifetimes were obtained with the same equipment as that operated in single-photon mode by using a 407-nm laser diode excitation controlled by a Hamamatsu C4725 stabilized picosecond light pulser. Analysis of the luminescence decay was accomplished by using software provided by the manufacturer. The lifetime values were obtained with an estimated uncertainty of 10%.

The vibronic band profiles of the corrected luminescence spectra, $I(E)$, on an energy scale (E, cm^{-1}) are analyzed according to eq 2, describing the relationship between the Franck−Condon envelope and some pertinent parameters.[46,47]

$$I(E) = \sum_m \sum_l \left(\frac{E_0 - m\hbar\omega_m - l\hbar\omega_l}{E_0}\right)^3 \frac{S_m^m}{m!}\frac{S_l^l}{l!} \times \exp\left[-4(\ln 2)\left(\frac{E - E_0 + m\hbar\omega_m + l\hbar\omega_l}{\Delta\bar{\nu}_{1/2}}\right)^2\right] \qquad (2)$$

with

$$S_j = \frac{\lambda_j}{\hbar\omega_j} \qquad (j = m \text{ and } l)$$

In this equation, E_0 is the energy of the 0−0 transition (the energy gap between the 0−0 vibrational levels in the excited and ground states), m and l are vibrational quantum numbers for high- and low-frequency modes, $\hbar\omega_m$ and $\hbar\omega_l$ (in practice, upper limits m and l = 5 are employed), $\Delta\bar{\nu}_{1/2}$ is the width at half-maximum of the vibronic band, λ and S are the reorganization energy and the displacement parameter along those modes, and k_B is the Boltzmann constant. High values for S_m (typically >0.7)[48] indicate that the excited state is significantly distorted along the concerned vibrational mode because of electronic *localization* effects. When the excited state undergoes extended electronic *delocalization*, low S_m values are obtained (typically in the range 0.2−0.6),[49] indicating that the electronic curve for the excited level is not much displaced relative to that for the ground state.

Synthesis. $[Ru(bpy)(eil)_2][PF_6]_2$ (2). $[Ru(bpy)Cl_3]_n$ (8.4 mg, 0.022 mmol) and **1** (15.0 mg, 0.042 mmol) were added to 5 mL of ethylene glycol and heated to 120 °C for 6 h under an argon atmosphere. The green reaction mixture obtained was cooled to room temperature, and a saturated KPF_6(aq) solution was added until precipitation of a green solid occurred. The solid was isolated by centrifugation and washed several times with water to remove traces of salts. The solid was dried in vacuo and then purified by chromatography on a Sephadex LH-20 column with 5:1 CH_3CN/CH_3OH as the eluent. Evaporation to dryness of the appropriate fraction yielded the desired green solid. Yield: 73% (19.4 mg). Anal. Calcd (found) for $C_{58}H_{32}F_{12}N_{10}P_2Ru\cdot 8H_2O$: C, 49.61 (49.84); H, 3.45 (3.07); N, 9.98 (9.84). ^{1}H NMR (400 MHz, CD_3CN, 295.8 ± 0.1 K, 0.756 mM): δ 8.826 (d, 1H, $J = 8.1$ Hz, H^c), 8.717 (d, 1H, $J = 6.4$ Hz, H^b), 8.652 (d, 1H, $J = 7.9$ Hz, $H^{c'}$), 8.612 (d, 1H, $J = 8.0$ Hz, H^3), 8.495 (d, 1H, $J = 6.5$ Hz, $H^{b'}$), 8.452 (d, 1H, $J = 8.0$ Hz, H^f), 8.390 (d, 1H, $J = 7.3$ Hz, $H^{f'}$), 8.274 (d, 1H, $J = 6.5$ Hz, H^a), 8.257 (d, 1H, $J = 6.5$ Hz, $H^{a'}$), 8.144 (t, 1H, $J = 7.9$ Hz, H^e), 8.125 (dt, 1H, $J = 6.5$ and 1.3 Hz, H^4), 8.060 (t, 1H, $J = 8.2$ Hz, $H^{e'}$), 8.030 (t, 1H, $J = 8.0$ Hz, H^d), 7.963 (d, 1H, $J = 5.6$ Hz, H^6), 7.896 (t, 1H, $J = 8.0$ Hz, $H^{d'}$), 7.422 (t, 1H, $J = 6.3$ Hz, H^5). ^{13}C NMR (CD_3CN, 298 K): δ 153.8 ($C-H^6$), 151.8 ($C-H^{a'}$), 150.8 ($C-H^a$), 139.1 ($C-H^4$), 134.1 ($C-H^e$), 133.6 ($C-H^{e'}$), 133.2 ($C-H^{f'}$), 133.0 ($C-H^f$), 132.0 ($C-H^d$), 131.8 ($C-H^{d'}$), 128.8 ($C-H^5$), 126.1 ($C-H^3$), 125.9 ($C-H^c$), 125.8 ($C-H^{c'}$), 122.9 ($C-H^b$), 122.7 ($C-H^{b'}$). FABMS: 970.2 $[M - 2PF_6 + H]^+$, 1115.1 $[M - PF_6 + H]^+$.

$[Ru(eil)_3][PF_6]_2$ (3). A suspension of *trans*-$[RuCl_2(py)_4]$ (11 mg, 0.023 mmol) and **1** (27 mg, 0.072 mmol) in 5 mL of deoxygenated ethylene glycol was stirred for 4 h at 120 °C under an argon atmosphere. The color of the reaction mixture changed from orange to dark green. The dark green complex was precipitated by adding a saturated aqueous solution of KPF_6 to the reaction mixture. The complex was purified by repeated washings with a chloroform/methanol (1:1, v/v) solution and precipitation with diethyl ether. Typical yields were higher than 95%. Alternatively, the complex was prepared by the reaction of $RuCl_3\cdot nH_2O$ with 3+ equiv of **1** in deoxygenated ethylene glycol, which was stirred for 6 h at 145 °C and was obtained in a good yield, or by the reaction of $[RuCl_2(DMSO)_4]$ with 3+ equiv of **1** in deoxygenated ethylene glycol, which was stirred for 4 h at 135 °C. Anal. Calcd (found) for $C_{72}H_{36}F_{12}N_{12}P_2Ru\cdot 4H_2O$: C, 56.44 (56.75); H, 2.89 (3.25); N, 10.97 (10.70). ^{1}H NMR (500 MHz, DMSO-d_6): δ 8.96 (d, $J = 7.8$ Hz, 1H, H^c), 8.91 (d, $J = 6.2$ Hz, 1H, H^b), 8.62 (d, $J = 7.6$ Hz, 1H,

(43) Yeh, A. T.; Shank, C. V.; McCusker, J. K. *Science* **2000**, *289*, 935.
(44) Nakamaru, K. *Bull. Chem. Soc. Jpn.* **1982**, *55*, 2967.
(45) Demas, J. N.; Crosby, G. A., *J. Phys. Chem.*, **1971**, *75*, 991.
(46) Claude, J. P.; Meyer, T. J. *J. Phys. Chem.* **1995**, *99*, 51.
(47) Barkawi, K. R.; Murtaza, Z.; Meyer, T. J. *J. Phys. Chem.* **1991**, *95*, 47.
(48) Goze, C.; Chambron, J. C.; Heitz, V.; Pomeranc, D.; Salom-Roig, X. J.; Sauvage, J. P.; Morales, A. F.; Barigelletti, F. *Eur. J. Inorg. Chem.* **2003**, 3752.
(49) Hammarström, L.; Barigelletti, F.; Flamigni, L.; Armaroli, N.; Sour, A.; Collin, J. P.; Sauvage, J. P. *J. Am. Chem. Soc.* **1996**, *118*, 11972.

Scheme 1. Synthesis and Proton Numbering of **2**

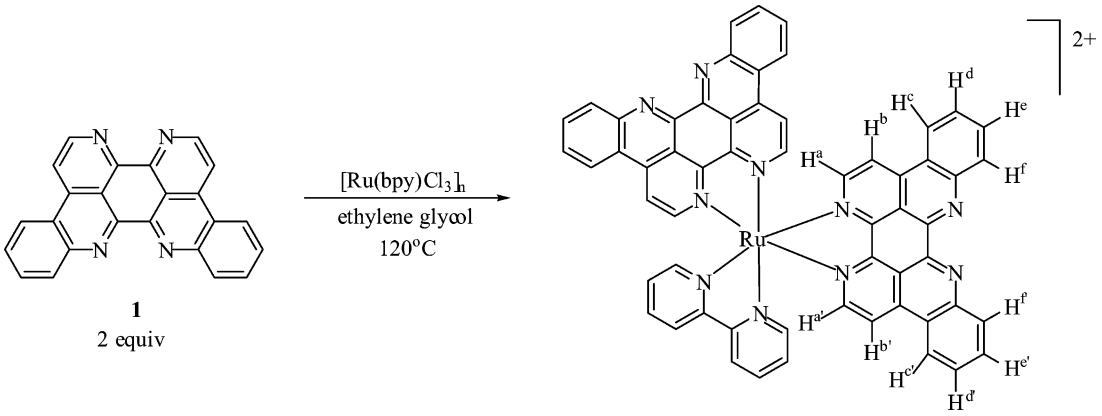

H^f), 8.40 (d, J = 6.2 Hz, 1H, H^a), 8.16 (t, J = 7.6 Hz, 1H, H^e), 8.01 (t, J = 7.6 Hz, 1H, H^d). ^{13}C NMR: δ 152.2 ($C-H^a$), 134.9 ($C-H^e$), 133.7 ($C-H^f$), 131.9 ($C-H^d$), 125.7 ($C-H^c$), 123.6 ($C-H^b$). FABMS: 1316 $[M - PF_6 + H]^+$, 1172 $[M - 2PF_6 + 2H]^+$.

$[Os(eil)_3][PF_6]_2$ (4). A suspension of *trans*-$[OsCl_2(py)_4]$ (15 mg, 0.026 mmol) and **1** (40 mg, 0.11 mmol) in deoxygenated ethylene glycol was stirred for 6 h at 120 °C under an argon atmosphere. The dark green complex was precipitated by the addition of a saturated aqueous solution of KPF_6. The purification was achieved by dissolving the complex in a minimal amount of a 1:1 DMSO/methanol solution and precipitation with diethyl ether. Yield: approximately 40%. Alternatively, the complex was prepared by the reaction of K_2OsCl_6 with 5+ equiv of **1** in deoxygenated ethylene glycol, which was stirred for 6 h at 150 °C and was obtained in a low yield. Anal. Calcd (found) for $C_{72}H_{36}F_{12}N_{12}P_2Os \cdot H_2O \cdot 2C_2H_6SO$: C, 52.96 (53.26); H, 2.92 (3.32); N, 9.75 (9.43). ^{1}H NMR (500 MHz, DMSO-d_6): δ 8.93 (d, J = 7.9 Hz, 1H, H^c), 8.75 (d, J = 6.1 Hz, 1H, H^b), 8.58 (d, J = 8.0 Hz, 1H, H^f), 8.40 (d, J = 6.4 Hz, 1H, H^a), 8.11 (t, J = 7.3 Hz, 1H, H^e), 7.99 (t, J = 7.7 Hz, 1H, H^d). ^{13}C NMR: δ 148.0 ($C-H^a$), 131.3 ($C-H^e$), 130.0 ($C-H^f$), 128.6 ($C-H^d$), 122.6 ($C-H^c$), 120.9 ($C-H^b$). FABMS: 1405 $[M - PF_6 + H]^+$, 1261 $[M - 2PF_6 + 2H]^+$.

Results and Discussion

Syntheses and NMR Characterization. The bis(eilatin) complex **2** was prepared by reacting $[Ru(bpy)Cl_3]_n$ with 2 equiv of **1** in ethylene glycol at 120 °C, as shown in Scheme 1. This green complex was isolated as the PF_6^- salt and purified by size-exclusion chromatography. The formation of **2** is accompanied by reduction of the ruthenium center to an oxidation state of II. The ^{1}H NMR spectrum of the complex in CD_3CN exhibits 4 signals for the bpy ligand and 12 signals for the eilatin ligand, consistent with the C_2 symmetry of the complex. The selective head binding of the eil ligand was determined by NOESY spectra, which clearly demonstrated a NOE correlation between the head eil protons (H^a and $H^{a'}$) and the bpy H^6 proton, as shown in Figure 1.

The ^{1}H NMR spectra of **2** in CD_3CN vary with concentration and temperature. The eil protons exhibit downfield shifts up to 0.43 ppm upon dilution over the concentration range 0.1−1 mM. The bpy protons shift upfield and to a lesser extent, i.e., up to 0.11 ppm, upon dilution over the same concentration range. This is consistent with $\pi-\pi$ stacking of the eil moieties of the complex. Raising the temperature has the same effect on the chemical shifts as dilution; both cause breaking of the intermolecular π-stacking interactions. This phenomenon was previously noted for complexes containing a single eilatin-type ligand of the general formula $[M(bpy)_2(Lig)]^{2+}$ (M = Ru, Os; Lig = eilatin, dibenzoeilatin, isoeilatin), which were shown to form discrete dimers in solution held by π-stacking interactions via the eilatin-type ligand.[28,30,31] However, because complex **2** contains two eilatin ligands, it is not restricted to dimer formation alone; instead, it has the potential to form various higher-order aggregates in solution. A comparison of **2** and the analogous mono(eilatin) complex $[Ru(bpy)_2(eil)][PF_6]_2$ (**5**),[28] which exhibits much larger concentration-induced shifts (up to ca. 1 ppm for identical protons over the same concentration range), implies that the π-stacking process is different for the two complexes. Both concentration-dependent ^{1}H NMR spectral data[50] and NMR diffusion measurements[51] do not give a conclusive picture as to the distribution of the various species in solution.

The tris(eilatin) complex **3** could be prepared in good yield

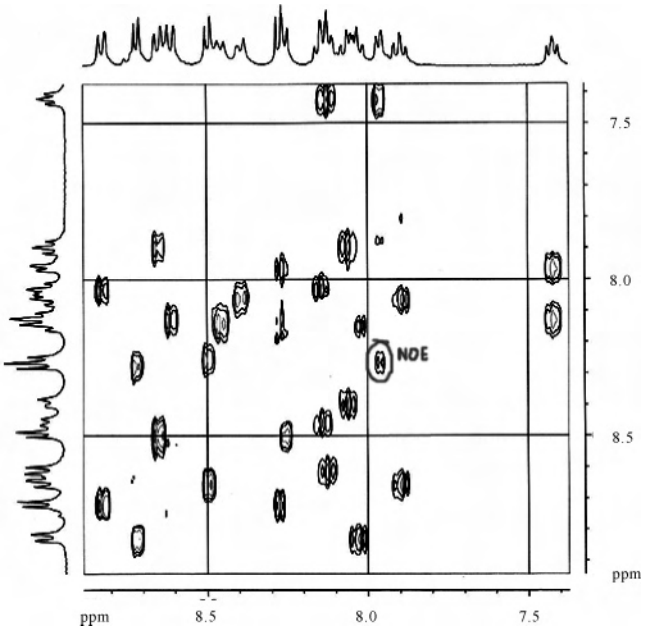

Figure 1. NOESY spectrum of **2**, recorded in CD_3CN. The NOE correlation between the bpy proton H^6 and the eil protons H^a and $H^{a'}$ is marked in gray.

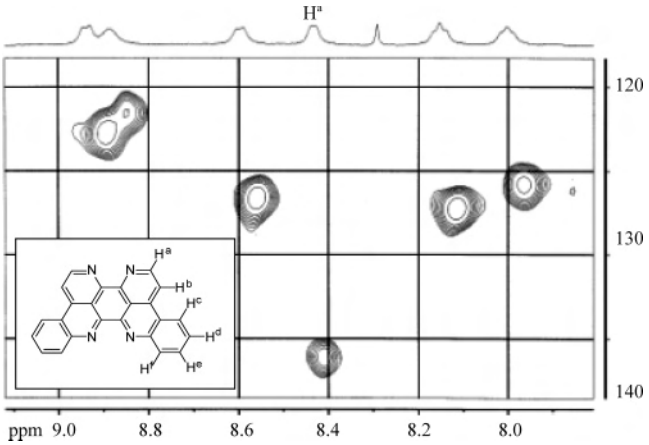

Figure 2. HSQC spectrum of complex **3**, recorded in DMSO-d_6.

by reacting 3+ equiv of **1** with a number of metal precursors, such as $[RuCl_3]\cdot nH_2O$, *trans*-$[RuCl_2(DMSO)_4]$, and *trans*-$[RuCl_2(py)_4]$. To the best of our knowledge, the latter has not been utilized as a synthetic precursor in the preparation of tris-bidentate polypyridyl complexes of ruthenium. The product was obtained as a dark green compound, isolated as the PF_6^- salt and purified by repeated washings with a 1:1 solution of chloroform and methanol to remove excess free ligand. The analogous osmium(II) complex **4** was similarly prepared by reacting 5+ equiv of **1** with K_2OsCl_6, *trans*-$[OsCl_2(DMSO)_4]$, or *trans*-$[OsCl_2(py)_4]$. The latter gave the desired product in much higher yield and under milder reaction conditions. The product, a dark green compound, was isolated as the PF_6^- salt and purified by dissolving the crude product in a minimal volume of a 1:1 DMSO/methanol solution and precipitation with ether.

^{1}H NMR spectra of complexes **3** and **4** in DMSO-d_6 exhibit six signals, consistent with the expected D_3 symmetry of a tris(eilatin) complex. FABMS and elemental analysis further support the formation of the tris complexes. By employing ^{1}H COSY, NOESY, and HSQC NMR techniques, we were able to elucidate the structure of the product: the C−H^a group is identified in the HSQC spectrum because this group, which is located next to the aromatic nitrogen, exhibits a low-field signal in the ^{13}C NMR spectrum (demonstrated for complex **3**; see Figure 2). The H^a proton in the complexes (8.43 ppm for **3** and 8.40 ppm for **4)** is shifted to a higher field relative to the same proton in the free ligand (9.18 ppm for free eilatin). We attribute this shift to ring currents that originate from the adjacent perpendicular aromatic rings. Thus, complexes **3** and **4** are indeed the tris-(homoleptic) complexes in which the eilatin ligands bind through their less hindered bpy-type head. This "triple" selectivity in binding is maintained *regardless* of the metal precursor employed in the synthesis.

Absorption Spectra. The UV/vis spectra of all of the complexes were recorded in acetonitrile; absorption spectra for complexes **2** and **5** are illustrated in Figure 3 together with that for **1**. Absorption data listing energy maxima and

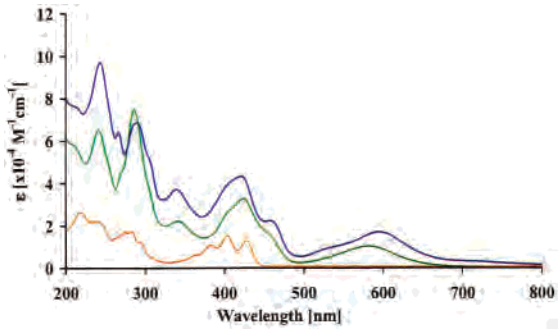

Figure 3. Absorption spectra of the complexes **2** (blue line) and **5** (green line), and of **1** (yellow line), recorded in acetonitrile.

Table 1. Absorption Data[a]

compd	absorption maxima λ_{max}, nm ($10^{-4}\epsilon$, M^{-1} cm^{-1})
1[b]	242(4.8), 286(3.7), 360(1.1), 388(2.1), 408(3.0), 434(2.7)
5[c,d]	241(6.8), 286(7.3), 341(2.2), 405sh, 424(3.3), 460sh, 583(1.0)
6[d]	242 (5.6), 289 (6.4), 355 (1.9), 418 (2.3), 450 sh, 612 (0.9)
2	243(9.7), 266(7.1), 289(7.2), 339(3.8), 420(4.4), 457(2.3), 594(1.7)
3[e]	242, 293, 337, 405, 424, 460, 595
4[e]	244, 296, 340, 408, 432(sh), 462(sh), 632

[a] Recorded in acetonitrile. [b] From ref 56 in methanol. [c] From ref 27. [d] From ref 28. [e] Solubility problems prevented the determination of the extinction coefficient, ϵ.

absorption coefficients are summarized in Table 1. The assignments of the absorption bands were based on the previously assigned optical transitions of **5** and $[Os(bpy)_2(eil)][PF_6]_2$ (**6**),[27−29] as discussed below.

We have previously reported that the absorption spectrum of the complex **5** contains intense absorption bands in the UV region (200−350 nm), assigned to ligand-centered $\pi \rightarrow \pi^*$ transitions of the peripheral bpy ligands; absorption centered around 420 nm, assigned to eilatin-centered $\pi \rightarrow \pi^*$ transitions**,** overlapping with $d_\pi(M) \rightarrow \pi^*$(bpy) MLCT transitions; and a broad, low-lying absorption band centered around 600 nm, assigned to $d_\pi(M) \rightarrow \pi^*$(eil) MLCT transitions.[27,29] The combination of absorptions at 600 and 420 nm renders this complex its dark green color. Upon sequential addition of eil ligands, the transitions involving the bpy ligands decrease in intensity, whereas the transitions involving the eil ligands increase in intensity. In addition, there is a slight red-shifting of the $d_\pi(M) \rightarrow \pi^*$(eil) MLCT transition, occurring at 583 nm for **5**, 591 nm for **2**, and 599 nm for **3.** An additional red-shifting of the $d_\pi(M) \rightarrow \pi^*$(eil) MLCT transition is observed on going from **3** to **4** (599 and 632 nm, respectively), as expected of the higher-lying d_π-(Os) orbitals.

Electrochemistry. While the redox behavior of the mono-(eilatin) complexes $[M(N-N)_2(eil)]^{2+}$ has been studied extensively,[29] the low solubility of the bis- and tris(eilatin) complexes did not allow their electrochemical characterization in 0.1 M TBAH/acetonitrile. We therefore performed cyclic and square-wave voltammetry measurements of these complexes (as well as of the mono(eilatin) complex **5**, for comparison) in DMSO.[52] The tendency of eilatin complexes to aggregate in an acetonitrile solution is diminished in DMSO,[27] and therefore these complexes are highly soluble

(50) Fielding, L. *Tetrahedron* **2000**, *56*, 6151.
(51) Gafni, A.; Cohen, Y. *J. Org. Chem.* **1997**, *62*, 120.

Table 2. Half-Wave Potentials for the Reduction of the Complexes[a]

complex	eil$^{0/-}$		eil$^{-/2-}$		bpy$^{0/-}$		
$[Ru(bpy)_3][PF_6]_2$					−1.71 (80)	−1.89 (60)	−2.15 (70)
2	−0.84[b]	−0.96[b]	−1.37[b]	−1.52[b]		−2.16 (70)	
5	−0.88 (100)[c]		−1.34 (70)		−1.91 (70)		−2.16 (70)

[a] Potentials are given vs the Fc/Fc^+ couple in DMSO, with 0.1 M TBAH as the supporting electrolyte, measured at room temperature with a scan rate of 0.1 V/s; ΔE_p values in mV are given in parentheses. [b] Values determined from square-wave voltammetry. [c] The relatively large ΔE_p value results from residual π-stacking-induced dimerization in DMSO/0.1 M TBAH; in acetonitrile, where substantial dimerization occurs, this reduction wave appears split into two waves of half-intensity.[29]

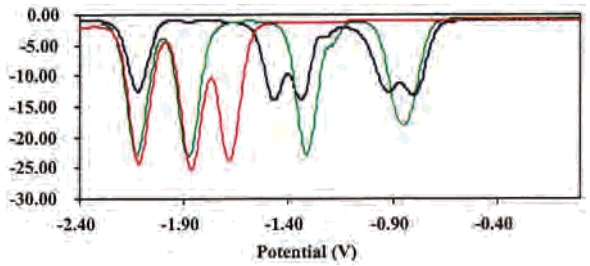

Figure 4. Square-wave voltammograms of **2** (blue line), **5** (green line), and $[Ru(bpy)_3][PF_6]_2$ (red line) vs $Ag/AgNO_3$.

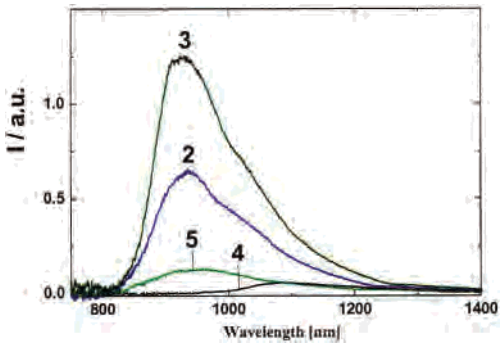

Figure 5. Corrected emission spectra of the indicated complexes at room temperature in an air-equilibrated CH_3CN solvent, from excitation of isoabsorbing solutions at $\lambda_{exc} = 460$ nm.

in this particular medium, even in the presence of the TBAH electrolyte. However, the redox window of DMSO is rather narrow (because of facile oxidation of this solvent), and therefore only the reduction processes could be characterized. While the change of the medium was beneficial for **2**, the electrochemical measurements for the tris(eilatin) complexes were unsuccessful because of desorption complications. The data for complexes **2** and **5**, together with the data measured for $[Ru(bpy)_3][PF_6]_2$ for comparison purposes, are collected in Table 2; representative square-wave voltammograms are shown in Figure 4.

The voltammograms exhibit several interesting features: (i) Several reduction processes of the eilatin complexes are substantially anodically shifted with respect to $[Ru(bpy)_3][PF_6]_2$ and are therefore assigned to reduction of the eil moieties. (ii) Each eil moiety can accept up to two electrons, as observed clearly for **5**. (iii) Because of the close proximity of the eil ligands in **2**, they do not undergo a two-electron reduction at the same potential; instead, two closely spaced one-electron reductions are observed, for both the first and second processes. (iv) Additional reduction processes, occurring at further negative potentials, are assigned to reductions of the bpy ligands. The number of such reductions is in accordance with the number of bpy ligands present in the complex, and the potentials are in perfect agreement with those of the $[Ru(bpy)_3]^{2+}$ complex.

Luminescence and Photophysics. The emission spectra of the complexes as the PF_6^- salts were recorded at room temperature in an acetonitrile solution and at 77 K (in a frozen solvent). The luminescence spectra for **2**−**5** are depicted in Figure 5; emission band maxima (λ_{max}), emission quantum yield (Φ), and lifetime (τ) values are collected in Table 3, together with data for $[Ru(bpy)_3]^{2+}$. The luminescence quantum yields, lifetimes, and spectral profiles are all consistent with a ^{3}MLCT nature for the excited state responsible for the emission; this is also indicated by the blue shifts on passing from room temperature to 77 K.

Table 3. Luminescence and Photophysical Properties of $[Ru(bpy)_x(eil)_y]^{2+}$ ($x + y = 3$) and $[Os(eil)_3]^{2+}$ [a]

	298 K					77 K	
complex	λ_{max} (nm)	Φ	τ (ns)	$10^{-4}k_r$ (s^{-1})	$10^{-7}k_{nr}$[c] (s^{-1})	λ_{max} (nm)	τ (μs)
$[Ru(bpy)_3]^{2+}$	653[b]	0.062	900 (170)	6.9	0.1	634[b]	5.0
5	945	4.4×10^{-4}	35 (30)	1.3	2.9	908	2.3
2	932	2.0×10^{-3}	65 (50)	3.1	1.5	893	2.3
3	926	4.6×10^{-3}	120 (80)	3.8	0.83	870	2.3
4	1087	1.4×10^{-4}	*d*	*d*	*d*	982	*d*

[a] In a degassed CH_3CN solution, at 298 and 77 K; in parentheses are values for air-equilibrated solutions; $\lambda_{exc} = 460$ nm (luminescence spectra) or 407 nm (luminescence lifetimes; see text). [b] Values obtained with the employed IR fluorimeter (see the Experimental Section) are slightly different from those from previous reports, for instance, see ref 32. [c] From $k_r = \Phi/\tau$ and $k_{nr} = 1/\tau - k_r$. [d] Too weak to detect.

As observed for the absorption spectra, for the examined series of Ru(II) complexes at room temperature, substitution of eil for bpy results in the shifting of the emission maxima to lower energies compared to $[Ru(bpy)_3]^{2+}$, leading to emission peaks at 945, 932, and 926 nm for the mono- (**5**), bis- (**2**), and tris(eilatin) (**3**) ruthenium(II) complexes, respectively. This indicates that, upon passing from $[Ru(bpy)_3]^{2+}$ to **5**, **2**, and **3**, the charge-transfer nature of the emission changes from Ru → bpy to Ru → eil. It can be noticed that the emission wavelength decreases along the **5**, **2**, and **3** series (both at room temperature and at 77 K) and that both the lifetimes and quantum yields increase; see Table 3. For ruthenium(II) polypyridine complexes, it is well-

(52) For examples of electrochemical measurements in DMSO of Ru(II) complexes, see: (a) Winkler, K.; McKnight, N.; Fawcett, W. R. *J. Phys. Chem. B* **2000**, *104*, 3575. (b) McCarthy, H. J.; Tocher, D. A. *Inorg. Chim. Acta* **1989**, *158*, 1. (c) Neyhart, G. A.; Hupp, J. T.; Curtis, J. C.; Timpson, C. J.; Meyer, T. J. *J. Am. Chem. Soc.* **1996**, *118*, 3724. (d) Ennix, K. S.; McMahon, P. T.; de la Rosa, R.; Curtis, J. C. *Inorg. Chem.* **1987**, *26*, 2660. (e) Mizuno, T.; Wei, W.-H.; Eller, L. R.; Sessler, J. L. *J. Am. Chem. Soc.* **2002**, *124*, 1134. (f) McDevitt, M. R.; Addison, A. W. *Inorg. Chim. Acta* **1993**, *204*, 141.

known that the luminescence features are influenced by the energy gap between the luminescent level, ^{3}MLCT, and a higher-lying metal-centered level, ^{3}MC, of dd origin.[1,21] The energy position of the latter is not expected to change in the examined Ru-based complexes because the coordination properties of bpy and eil are not much different. On this basis, enhanced stabilization of the ^{3}MLCT level for **5**, **2**, and **3** as compared to $[Ru(bpy)_3]^{2+}$ is expected to result in an increased ^{3}MLCT−^{3}MC energy gap, thus depressing thermal population of the upper-lying ^{3}MC level, known to offer a rather effective way to nonradiative deactivation processes.[2,3,12,18b,21] As a consequence, for **5**, **2**, and **3**, only nonradiative paths governed by the energy-gap law (i.e., the gap between the luminescent level and the ground state)[19,53] should be taken into account.

A closer look at the balance between radiative and nonradiative processes for deactivation of the emissive levels provides interesting hints. Actually, from the quantum yields and lifetimes collected in Table 3, one can evaluate rate constants for the radiative (k_r) and nonradiative (k_{nr}) processes (eq 3).

$$k_r = \Phi/\tau \tag{3a}$$

$$k_{nr} = 1/\tau - k_r \tag{3b}$$

On this basis, one can notice that the values for k_r listed in Table 3 are in accord with expectations based on the known relationship between k_r and the average emissive level (eq 4),[54] where n, $\vec{M}$, and $\langle\bar{\nu}\rangle$ are the refractive index of the

$$k_r/n^3 \propto |\vec{M}|^2\langle\bar{\nu}\rangle^3 \tag{4}$$

solvent, the transition moment, and the average emissive level (approximated here by the energy value at the peak maximum) on an energy scale (cm^{-1}), respectively.

On the other hand, according to the energy-gap law (eq 5) and for a sufficiently high ^{3}MLCT−^{3}MC energy gap, k_{nr} is likewise expected to be related to the emissive energy level.[19−23,53,54] Here, S_m is the displacement parameter (the

$$\ln(k_{nr}) \propto -S_m - \gamma\frac{E_0'}{\hbar\omega_m} \tag{5}$$

electronic−vibrational coupling constant or Huang−Rhys coupling constant; see the Experimental Section), along a high-frequency (m) vibrational mode, $\hbar\omega_m$, the relevant energy level is $E_0' = E_0 + S_l\hbar\omega_l$, with $\gamma = \ln[E_0'/(S_m\hbar\omega_m) - 1]$, and S_l and $\hbar\omega_l$ refer to low-frequency (l) modes. Indeed, a decrease in k_{nr} is observed along the **5**, **2**, and **3** series (Table 3), and the trend in the k_{nr} values agrees with predictions based on eq 5.

It is interesting that, by fitting eq 2 of the Experimental Section to the luminescence spectra, one can estimate values for E_0, λ, and S along the vibrational modes that contribute to deactivation of the excited level. Results for the luminescence profiles of the series $[Ru(bpy)_x(eil)_y]^{2+}$ ($x + y = 3$), as obtained at 77 K, are shown in Figure 6 and collected in Table 4. In particular, the low S_m values for complexes **5**, **2**, and **3** ($S_m \sim 0.5$ and $\hbar\omega_m = 1300$ cm^{-1}; see Table 4) suggest that the electronic curve for the emissive level is not much displaced relative to that for the ground state.[1] This effect is due to the effective electronic delocalization at a large size ligand,[15,48,55] a consequence of the Ru → eil charge-transfer nature of the emission in **5**, **2**, and **3**.

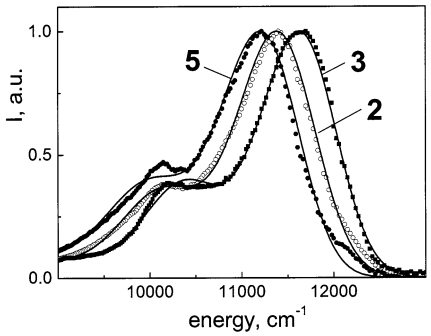

Figure 6. Vibronic analyses of the luminescence profiles in a frozen CH_3CN solvent at 77 K for the indicated complexes.

Table 4. Data from Vibronic Analysis of the Luminescence Spectra for the Complexes $[Ru(bpy)_x(eil)_y]^{2+}$ ($x + y = 3$)[a]

	E_0 (cm^{-1})	S_m[b]	$\hbar\omega_m$ (cm^{-1})	S_l[b]	$\hbar\omega_l$ (cm^{-1})	$\Delta\bar{\nu}_{1/2}$[c] (cm^{-1})
5	11380	0.49	1300	0.73	400	800
2	11490	0.47	1300	0.46	400	870
3	11730	0.51	1300	0.50	400	830

[a] According to eq 2 of the text, the solvent was CH_3CN, the temperature was 77 K, and excitation was performed at 460 nm. [b] Displacement parameter, $S = \lambda/\hbar\omega$, along high- (m) and low-frequency (l) vibrations; see the text. [c] Full width at half-maximum.

For the Os(II) complex, the emission occurs at even longer wavelengths (peak maximum at 1087 nm), as expected from the higher-lying metal-centered orbitals, which also leads to longer wavelength absorption (see above).

Conclusions

The series of complexes $[Ru(bpy)_x(eil)_y]^{2+}$ ($x + y = 3$) and the complex $[Os(eil)_3]^{2+}$ were designed with the intent of examining the effect of sequential substitution of eil for bpy on the electrochemical and photophysical properties. The absorption spectra of the complexes exhibit several bpy- and eil-associated $\pi-\pi^*$ and MLCT transitions, whose energy and relative intensity depend on the number of ligands bound to the metal center (x and y). Electrochemical measurements performed in DMSO reveal several ligand-based reduction processes, where each eil ligand can accept up to two electrons at potentials that are significantly anodically shifted with respect to the bpy ligands. Both at room temperature and at 77 K, the complexes exhibit near-IR emission of typical ^{3}MLCT character. For the series of complexes **5**, **2**, and **3**, the luminescence quantum yields and lifetimes are strictly governed by the balance between radiative and

(53) Freed, K. F.; Jortner, J. *J. Chem. Phys.* **1970**, *52*, 6272.
(54) Chen, P. Y.; Meyer, T. J. *Chem. Rev.* **1998**, *98*, 1439.
(55) Balazs, G. C.; del Guerzo, A.; Schmehl, R. H. *Photochem. Photobiol. Sci.* **2005**, *4*, 89.
(56) Rudi, A.; Benayahu, Y.; Goldberg, I.; Kashman, Y. *Tetrahedron Lett.* **1988**, *29*, 3861.

nonradiative processes, as established for MLCT emitters. These complexes join the still uncommon family of near-IR-emitting polypyridyl complexes.

Acknowledgment. This research was supported by the Israel Science Foundation founded by the Israel Academy of Sciences and Humanities and by the FIRB Project RBNE019H9K "Molecular Manipulation for Nanometric Devices" by MIUR. We thank Dvora Reshef for technical assistance.

Supporting Information Available: A plot of k_r and k_{nr} vs the emission level. This material is available free of charge via the Internet at http://pubs.acs.org.

IC051022V